Optics Communications 419 (2018) 47–52

Contents lists available at ScienceDirect

Optics Communications

journal homepage: www.elsevier.com/locate/optcom

Grating-lobe-suppressed optical phased array with optimized element distribution

Daocheng Zhang, Fangzheng Zhang *, Shilong Pan

Key Laboratory of Radar Imaging and Microwave Photonics, Ministry of Education, Nanjing University of Aeronautics and Astronautics, Nanjing 210016, China

ARTICLE INFO

Keywords:
Optical phased array (OPA)
Modified genetic algorithm
Grating lobe
Side lobe

ABSTRACT

A grating-lobe-suppressed optical phased array (OPA) is proposed to realize optical beam steering based on unequally-spaced technique, in which the element distribution is optimized by a modified genetic algorithm to achieve a minimum peak side-lobe level (PSLL). Numerical simulations of one-dimensional (1-D) and two-dimensional (2-D) OPAs are carried out. The results show that by optimizing the element distribution in an unequally-spaced OPA using the modified genetic algorithm, the grating lobes and side lobes can be well suppressed. Specifically, the PSLL of the far-field pattern reaches as low as 0.1 and 0.23 in 0° beam direction for a 1-D 20-element OPA and a 2-D 10 × 10 OPA, respectively, which is much better than the traditional unequally-spaced OPA. The relationship between the optimized PSLL and the practical fabrication accuracy is investigated. The results indicate that the proposed OPA can allow a certain fabrication deviation, and the PSLL can keep a low level within the whole scanning range of 180°, although a slightly higher PSLL is achieved for a larger beam angle. Besides, the simulations results also show that, the spacing range between adjacent elements and the element number should be appropriately chosen to achieve a better side-lobe-suppression and a narrow beam width.

1. Introduction

Optical phased array (OPA) is an optical beam steering technique that enables free-space fast beam scanning without moving or rotating the facilities. OPA has wide applications in laser radar, large size high-resolution display, and wide bandwidth free space optics communications, etc. [1–4]. Thanks to its much smaller wavelength compared with microwave phased arrays, OPAs have advantages of high resolution, secrecy and chip-scale. However, limited by the state-of-the-art fabrication levels, the realizable element interval of current OPA is much larger than half of the light wavelength, which results in the formation of many grating lobes in the far-field. Grating lobes are generated due to the periodicity in the radiation pattern and formed in directions where a maximum in-phase addition of radiated fields occurs [5]. The existence of large grating lobes would not only reduce the energy efficiency but also limit the beam scanning range. Consequently, grating lobes is a great challenge for OPA technology. In addition to grating lobes, the existence of side lobes would also degrade the quality of beam forming. Side lobes are the result of constructive and destructive interference from different radiating elements of the optical phased array. Up to now, a few methods have been proposed to suppress the side lobes or the grating lobes. Side lobe suppression can be achieved via amplitude or phase weighting. However, the grating lobes cannot be effectively suppressed through amplitude or phase weighting [5–7], because of the periodicity of the radiation pattern. Unequally-spaced phased array, in which the element distribution is not uniform, can be applied to effectively suppress the grating lobes. When an appropriate element distribution is adopted, amplitudes of the side lobes can also be suppressed. Feasibility of the unequally-spaced optical phased array for grating lobe suppression has been verified [8]. However, the ideal element distribution of an OPA for the best grating lobe suppression has not been investigated, which means that there is potential to further reduce the grating lobes based on an unequally spaced OPA.

In this paper, we propose and investigate an approach to suppress the grating lobes based on unequally-spaced phased array, in which a modified genetic algorithm is applied to search for an ideal element distribution. Using the modified genetic algorithm, the distribution of the phased array elements can be quickly optimized to largely suppress the grating lobes and side lobes. Performance of the proposed method is investigated though numerical simulations of one-dimensional (1-D) and two-dimensional (2-D) OPAs. The influence of practical fabrication accuracy on the optimized PSLL is also investigated. In addition, the relationship between the peak side-lobe level (PSLL) of one-dimensional

* Corresponding author.
E-mail address: zhangfangzheng@nuaa.edu.cn (F. Zhang).

https://doi.org/10.1016/j.optcom.2018.03.007
Received 25 September 2017; Received in revised form 22 February 2018; Accepted 5 March 2018

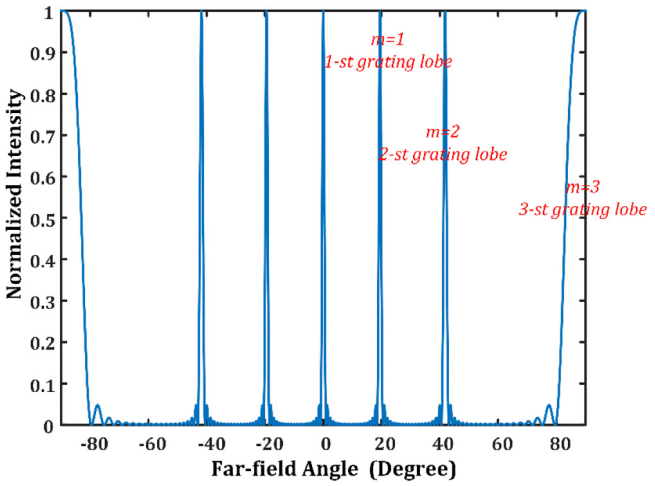

Fig. 1. The simulated far-field pattern of a uniform OPA with an inter-element spacing of 3λ.

OPA and the beam angle is analyzed, and the optical beam width is also compared under different parameters.

2. Principle

In a typical uniform 1-D OPA that consists of N phase elements with an inter-element spacing of d, when all the array elements have the same emission amplitude A, the far-field light intensity can be expressed as [5]

$$I(\theta) = |E(\theta)|^2 = A^2 \frac{\sin^2[N\frac{\pi}{\lambda}d(\sin\theta - \sin\theta_s)]}{\sin^2[\frac{\pi}{\lambda}d(\sin\theta - \sin\theta_s)]} \tag{1}$$

where λ, θ and θ_s denotes the optical wavelength, the observation direction and the scanning angle of the beam, respectively. Based on (1), the angle corresponding to the main lobe is θ_s, and the angle of the grating lobes are determined by [9]

$$\theta_{grating-lobe} = \pm \arcsin\left(\frac{m\lambda}{d} + \sin\theta_s\right), \quad m = 1, 2, 3\ldots \tag{2}$$

where m denotes the order of grating lobes. Fig. 1 shows the far-field pattern of a uniform OPA with an equal inter-element spacing of 3λ, where grating lobes comparable with the main lobe are observed.

In an unequally-spaced OPA, the element spacing is not a constant. In this case, the grating lobes will not be the result of fully constructive interference from different radiating elements of the optical phased array. By appropriately choosing the element spacings, the grating lobes can be effectively suppressed. The far field of an unequally-spaced OPA can be expressed as:

$$E(\theta) = \sum_{n=1}^{N} E_n(\theta) = \sum_{n=1}^{N} A e^{j\frac{2\pi}{\lambda}x_n(\sin\theta - \sin\theta_s)}, \qquad x_n = \sum_{k=1}^{n-1} d_k. \tag{3}$$

where x_n represents the distance between the nth phase element and the 1st phase element, and d_k denotes the distance between the kth element and the $(k+1)$th element. In this case, the half power beam width (HPBW) of the main lobe is given by [9]

$$\theta_{3\,\mathrm{dB}} \approx \frac{1}{\cos\theta_s}\frac{0.866\lambda}{\sum_{k=1}^{N-1} d_k} \tag{4}$$

From Eq. (3), symmetry is found by

$$I(\theta)|_{\theta_s=\theta_0} = I(-\theta)|_{\theta_s=-\theta_0} \tag{5}$$

which means when the beam angles are symmetrical about 0°, the intensity distributions are symmetrical about 0° direction.

To achieve beam scanning in a semi-sphere, a two-dimensional (2-D) OPA should be constructed. Fig. 2(a) shows a 2-D unequally-spaced OPA. The phase elements are distributed non-uniformly on the x–y plane, which is the equator plane of a far-field spherical system, as shown in Fig. 2(b). The far-field expression of a 1-D unequally-spaced OPA can be extended to the 2-D case [9]:

$$\begin{aligned} E(\theta) &= \sum_{n=1}^{N} E_n(\theta) \\ &= \sum_{m=1}^{M}\sum_{n=1}^{N} e^{j\frac{2\pi}{\lambda}\cdot(x_m\sin\theta\cos\varphi + y_n\sin\theta\sin\varphi)} \cdot e^{-j\frac{2\pi}{\lambda}\cdot(x_m\sin\theta_s\cos\varphi_s + y_n\sin\theta_s\sin\varphi_s)} \end{aligned} \tag{6}$$

where (x_m, y_n) is the location of the phase element, θ and φ denotes the azimuth and elevation angles of the far-field pattern, respectively, and θ_s and φ_s are the azimuth and elevation angles of the beam, respectively.

To obtain an unequally-spaced OPA with minimized side-lobes, we propose to use a modified genetic algorithm to optimize the element spacings. The flowchart of the optimization algorithm is shown in Fig. 3. Implementing the modified genetic algorithm is a process of optimization, which consists of initialization, fitness evaluation, selection, crossover, mutation and termination [10]. Firstly, a set of initial inter-element spacings are generated randomly subjecting to the limitations of fabrication technology, and used as the chromosomes in the modified genetic algorithm. Then, a fitness evaluation is required to measure how good these chromosomes are at solving the problem. Here, the side-lobe suppression ratio is used for the fitness evaluation, which is represented by the peak side-lobe level (PSLL) defined by

$$PSLL = \frac{I_{\max\, sidelobe}}{I_{mainlobe}} \tag{7}$$

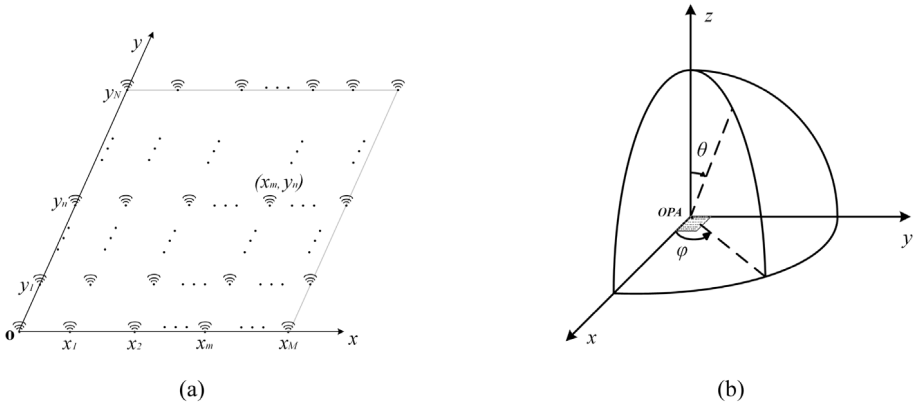

(a) (b)

Fig. 2. (a) Schematic illustration of a 2-D unequally-spaced OPA, and (b) an illustration of the far-field in a spherical system.

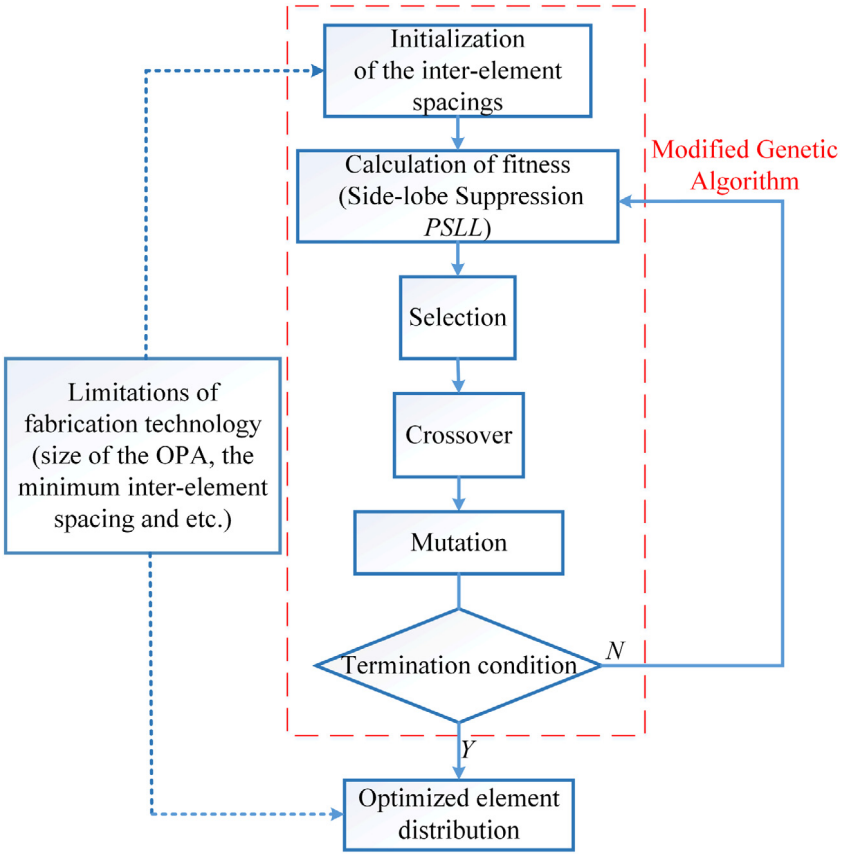

Fig. 3. Flowchart of the optimization algorithm.

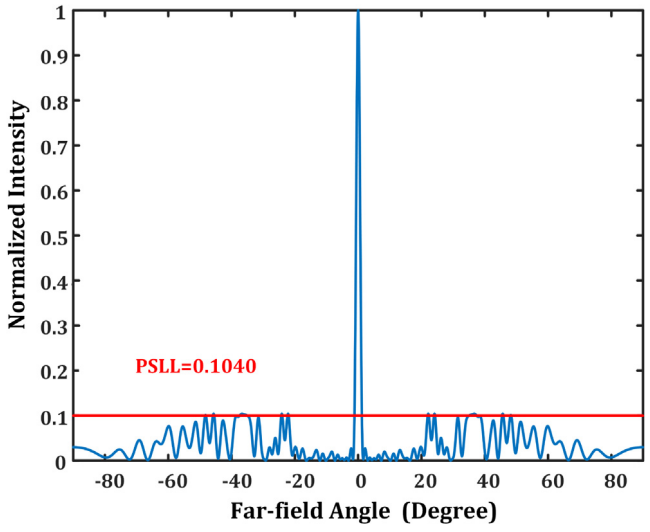

Fig. 4. The simulated far-field pattern of an unequally-spaced OPA with optimized element distribution (PSLL = 0.1040).

where $I_{\max\ sidelobe}$ is the maximum power of the side-lobe, and $I_{main\ lobe}$ is the power of the main lobe. In this case, the aim of the modified genetic algorithm is to search for the optimal element distribution to minimize PSLL of the OPA. To do this, a combination of selection, crossover and mutation is performed to search for the optimal solution by mimicking the same processes that nature uses [10]. The basic ideal of this process is to update the chromosomes through crossover and mutation based on selected pieces from the current chromosomes that may contribute to achieving a better fitness evaluation result. This optimization process is repeated until a desired number of cycles, or number of evolutionary generations has been reached. Validity of the initialization of inter-element spacings and the optimized element distribution should be verified with the limitations of the state-of-the-art fabrication technology, including the number of phase elements, size of the OPA and the minimum inter-element spacing.

For a 1-D unequally-spaced OPA, the optimization can be expressed as to find the inter-element spacings to minimize the PSLL by

$$\begin{cases} \min PSLL = f(d_1, d_2, \ldots, d_{n-1}) \\ s.t.\ \min\{d_1, d_2, \ldots, d_{n-1}\} \geq d_{\min}, \quad \sum_{k=1}^{n-1} d_k \leq D, k = 1, 2 \ldots, n-1. \end{cases} \tag{8}$$

where $d_{\min}$ is the minimum element spacing, D is the size of the OPA, n is the element number, and d_k is the distance between the kth and the $(k+1)$th element. For a 2-D unequally-spaced OPA, two-dimensional element distribution can also be optimized based on the same principle.

3. Simulation

To investigate the performance of the proposed method, simulations of the far-field optical intensity of a 1-D unequally-spaced OPA are carried out. In the simulation, the OPA consists of 20 elements and the operating wavelength (λ) is 1 μm. The emission amplitudes of all the elements are identical and the adjacent element spacing can be chosen arbitrarily between 1 μm and 3 μm (i.e., from λ to 3λ). In the simulation, the selection of computing parameters in the modified genetic algorithm is essential. After parameter optimization according to the grating-lobe suppression performance, the number of evolutionary generations, the population size, the crossover probability and the mutation probability is set to 300, 200, 0.8 and 0.02, respectively. Here, the crossover probability represents the chance that two chromosomes will swap their

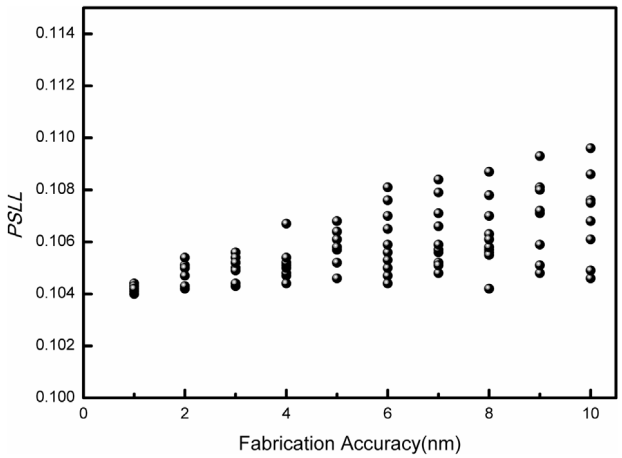

Fig. 5. Relationship between PSLL and fabrication accuracy.

bits, and the mutation probability is the chance that a bit within a chromosome will be flipped [10].

First of all, the far-field intensity of an unequally-spaced OPA with a beam angle of 0° is investigated. As we know, for the far-field pattern of a uniform OPA with a fixed element spacing larger than half of the light wavelength, strong grating lobes comparable with the main lobe are generated. For an unequally-spaced OPA of which the element distribution is optimized by the modified genetic algorithm, the far-field pattern is shown in Fig. 4, where the grating lobes are suppressed and a PSLL as low as 0.1040 is achieved. In this case, the theoretical optimized distance between adjacent elements of the 20-element OPA is 2.498 μm, 1.176 μm, 1.686 μm, 1.819 μm, 2.971 μm, 1.975 μm, 1.633 μm, 1.044 μm, 2.050 μm, 1.968 μm, 2.669 μm, 2.975 μm, 1.906 μm, 1.065 μm, 2.014 μm, 2.376 μm, 1.572 μm, 1.745 μm, and 2.338 μm. In practice, in case the distance between two elements cannot be guaranteed adequately accurate to achieve the ideal grating lobe suppression, further investigation of the relationship between the fabrication accuracy of the OPA and the grating suppression is necessary. Based on the CMOS technology, the state-of-the-art fabrication accuracy can reach sub-nanometer or nanoscale orders of magnitude [11]. Fig. 5 shows the PSLL obtained through multiple simulations when the element distance accuracy changes from 1 nm to 10 nm. It is shown that the PSLL of an optimized OPA with the modified genetic algorithm can be kept within 0.1040 and 0.1096 for a 10-nm fabrication accuracy. With the improvement of fabrication accuracy, the PSLL can further tend to the ideal PSLL, e.g., the PSLL is close to 0.1040 for a 1-nm fabrication accuracy. These results show that, the proposed OPA with modified genetic algorithm can allow a certain fabrication deviation.

Then, the results when the optical beam changes to other directions are calculated. Fig. 6(a), (b), (c) and (d) shows the far-field pattern of the optimized unequally-spaced OPA when the beam direction is at 15°, 30°, 45° and 60°, respectively. The corresponding PSLL is 0.1177, 0.1213, 0.1249 and 0.1269, respectively. These results show that by optimizing the element distribution of an unequally-spaced OPA, the grating lobes as well as the side lobes can be well suppressed.

In Fig. 6, the PSLL changes slightly as the beam direction changes. To check this property, simulations of an unequally spaced OPA with 10 phase elements are carried out. In the simulation, the light wavelength is still kept 1 μm, and the distance between adjacent elements are between 1 μm and 3 μm. The obtained PSLL of the optimized unequally-spaced OPA is shown by the circle markers in Fig. 7. As can be seen, within the scanning angular of 180°, PSLL of the optimized unequally-spaced OPA changes between 0.16 and 0.23. The best beam forming is achieved in the 0° direction. As the beam direction angle increases, the PSLL gets slightly larger. However, it is still kept within a low level within the

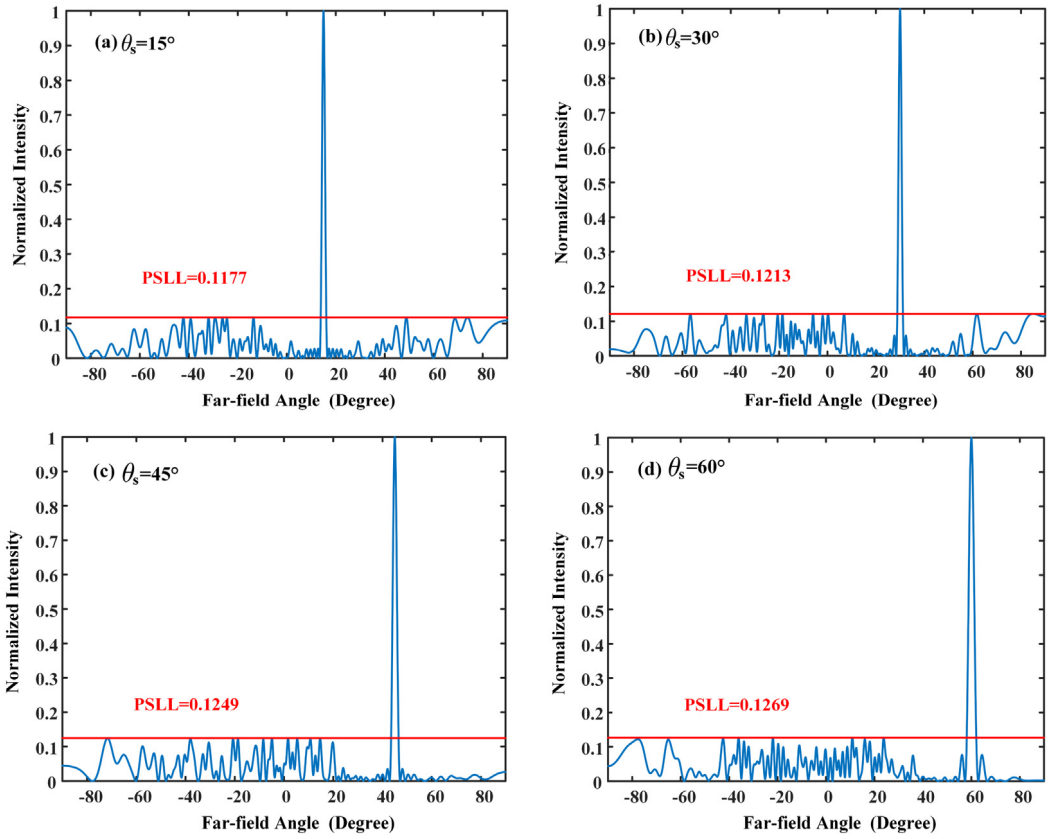

Fig. 6. The simulated far-field pattern of unequally-spaced OPAs with (a) θ_s = 15°, (b) θ_s = 30°, (c) θ_s = 45°, and (d) θ_s = 60°.

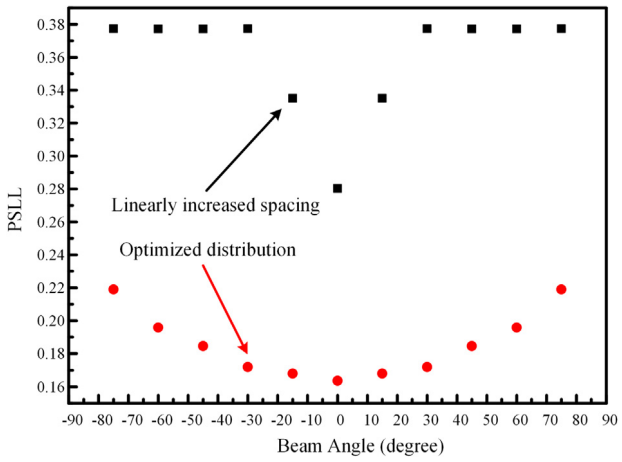

Fig. 7. Relationship between PSLL and beam angle (circle makers are results of OPA with optimized distribution, and square markers are the results of OPA with linearly increased spacing).

Table 1
PSLL and beamwidth of a 10-element OPA and a 20-element OPA.

Spacing range	PSLL		Beam width (rad)	
	10-elements	20-elements	10-elements	20-elements
1–3λ	0.1841	0.1040	0.0466	0.0231
3–10λ	0.2458	0.1588	0.0169	0.0072
10–20λ	0.3611	0.1969	0.068	0.0031

whole scanning range. As a comparison, the PSLL of an unequally-spaced OPA, of which the elemental spacing increases linearly from 1 μm to 3 μm, is calculated for different beam directions, as shown by the square markers in Fig. 7. In this case, the PSLL changes from 0.28 to 0.38, which is much larger than the PSLL of an optimized OPA. This result indicates that the side lobes can be better suppressed after optimizing the element distribution by the modified genetic algorithm.

The performance of an unequally-spaced OPA is related with the number of phase elements, and the achievable distance between adjacent elements. Table 1 shows the PSLL and beam width of the far-field pattern of a 10-element OPA and a 20-element OPA, of which the element distributions have been optimized by the modified genetic algorithm. In Table 1, different element spacing ranges are considered. As can be seen from Table 1, increasing the element spacing range can effectively compress the beam width, but the PSLL would get worse as the element space range is enlarged. Thus, a proper spacing range is required to achieve a tradeoff between the PSLL and beam width. On the other hand, when the element number is increased from 10 to 20, the PSLL gets better and the beam width is narrowed, leading to a better directionality. However, when choosing the element number in practice, the system complexity and cost should also be considered.

Finally, the far-field properties of a 2-D OPA are investigated. In the simulation, the 2-D OPA consists of 10 × 10 elements and the light wavelength is still 1 μm. The simulated far-field patterns of a 2-D OPA with beam direction of $\theta_s = 45°$ and $\varphi_s = 45°$ are shown in Fig. 8. Fig. 8(a) shows the far-field pattern of a uniform 2-D OPA with an element spacing of 1 μm. In this case, three grating lobes are generated. For an unequally-spaced 2-D OPA, of which the element spacings along x and y axes are optimized within 1 μm and 3 μm by the modified genetic algorithm, the far-field pattern is shown in Fig. 8(b). In the optimization process, the parameters in the modified genetic algorithm, including the number of evolutionary generations, the population size, the crossover probability and the mutation probability, are the same with the simulation in the 1-D OPA. In Fig. 8(b), the grating lobes are eliminated, and the side lobes are well suppressed with a PSLL as low as 0.23. Therefore, the proposed OPA design method is also feasible for 2-D OPA.

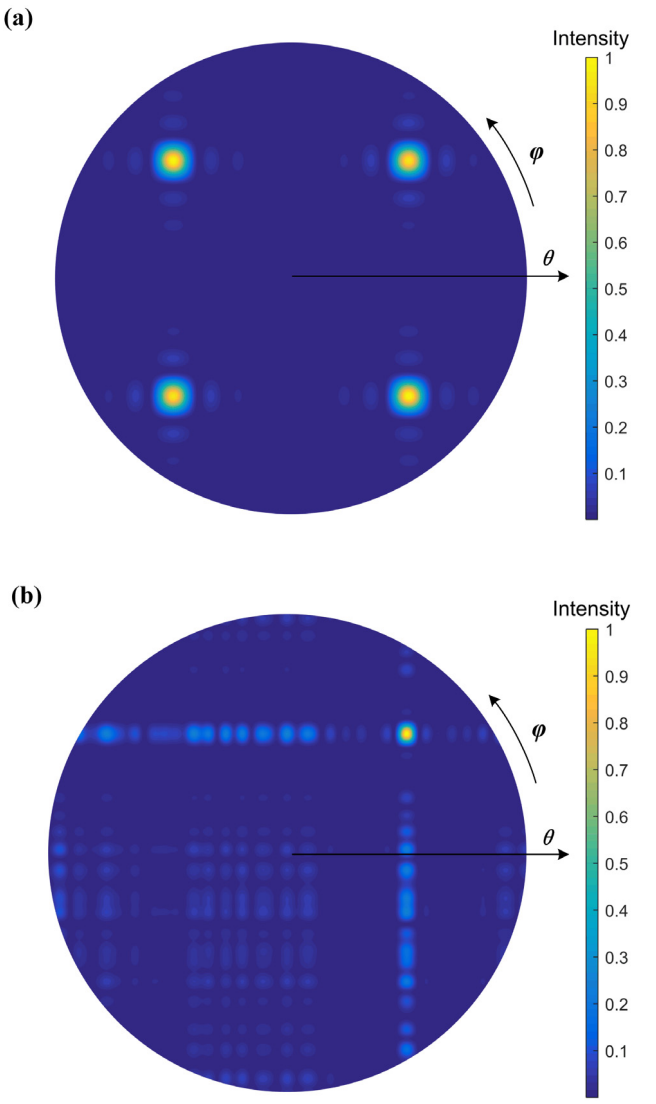

Fig. 8. Far-field patterns of (a) an equally-spaced 2-D OPA, and (b) an optimized unequally-spaced 2-D OPA.

4. Conclusions

We have proposed and investigated a grating-lobe-suppressed optical phased array (OPA) with its element distribution optimized by a modified genetic algorithm. Performance of the proposed OPA is analyzed through extensive numerical simulations. The results show that, the grating lobes and side lobes of an unequally-spaced OPA can be well suppressed after optimizing the element distributions. In the simulation, the PSLL reaches 0.1 and 0.23 in 0° direction for a 1-D 20-element OPA and a 2-D 10 × 10 OPA, respectively. And a certain fabrication deviation is allowed to achieve a good PSLL for the proposed OPA. In addition, although a slightly larger PSLL is achieved for a larger scanning angle, the PSLL is kept within a low level in the whole scanning range. Besides, the spacing range of adjacent elements, as well as the element number should be properly chosen considering the PSLL, the beam width, and the system complexity.

Acknowledgment

This work was supported in part by the NSFC program of China (61401201, 61422108).

References

[1] J. Montoya, A. Sanchez-Rubio, R.t. Hatch, H. Payson, Optical phased-array ladar, Appl. Opt. 53 (2014) 7551–7555.

[2] J. Sun, E. Timurdogan, A. Yaacobi, E.S. Hosseini, M.R. Watts, Large-scale nanophotonic phased array, Nature 493 (2013) 195–199.

[3] A. Linnenberger, S. Serati, J. Stockley, Advances in optical phased array technology, Proc. SPIE 6304 (2006) 63040T.

[4] A. Polishuk, S. Arnon, Communication performance analysis of microsatellites using an optical phased array antenna, Opt. Eng. 42 (2003) 2015–2024.

[5] H.J. Visser, Array and Phased Array Antenna Basics, John Wiley & Sons Inc., Hoboken, NJ, 2005.

[6] W. Huang, J. Montoya, J.E. Kansky, S.M. Redmond, G.W. Turner, A. Sanchez-Rubio, High speed, high power one-dimensional beam steering from a 6-element optical phased array, Opt. Express 20 (2012) 17311–17318.

[7] Y. Jin, A. Yan, Z. Hu, Z. Zhao, W. Shi, High speed and low side lobe optical phased array steering by phase correction technique, Proc. SPIE 8847 (2013) 884716.

[8] S. Yin, J.H. Kim, F. Wu, P. Ruffin, C. Luo, Ultra-fast speed, low grating lobe optical beam steering using unequally spaced phased array technique, Proc. SPIE 5911 (2007) 591104.

[9] C.A. Balanis, Antenna Theory: Analysis and Design, John Wiley & Sons Inc., 2016.

[10] J.H. Holland, Adaptation in Natural and Artificial Systems, University of Michigan Press, 1975.

[11] S.K. Selvaraja, W. Bogaerts, P. Dumon, Member, D.V. Thourhout, R. Baets, Subnanometer linewidth uniformity in silicon nanophotonic waveguide devices using CMOS fabrication technology, IEEE J. Sel. Top. Quantum Electron. 16 (2010) 316–324.